Exosomes derived from MDR cells induce cetuximab resistance in CRC via PI3K/AKT signaling-mediated Sox2 and PD-L1 expression

ZHENZHEN WEI[1,2*], ZIYUAN WANG[3*], QIONG CHAI[4], ZAN LI[1], MENGJIE ZHANG[1], YULI ZHANG[1], LU ZHANG[5], QINGFENG TANG[1], HUIRONG ZHU[2] and HUA SUI[1,2]

[1]Medical Experiment Center, Jiading Branch of Shanghai General Hospital, Shanghai Jiao Tong University School of Medicine, Shanghai 201803; Departments of [2]Medical Oncology and [3]Pathology, Shuguang Hospital; [4]Office of Academic Research, Shanghai University of Traditional Chinese Medicine, Shanghai 201203; [5]Department of Integrated Chinese and Western Medicine, The Affiliated Cancer Hospital of Zhengzhou University and Henan Cancer Hospital, Zhengzhou, Henan 450008, P.R. China

Received March 18, 2022; Accepted July 11, 2022

DOI: 10.3892/etm.2023.11785

Abstract. The anti-EGFR antibody cetuximab is used as a first-line targeted therapeutic drug in colorectal cancer. It has previously been reported that the efficacy of the EGFR antibody cetuximab is limited by the emergence of acquired drug resistance. In our previous study the transmissibility effect of exosomes from drug resistant tumor cells to sensitive tumor cells was identified. It can therefore be hypothesized that drug resistant cells might affect neighboring and distant cells via regulation of exosome composition and behavior. However, the mechanism of exosomes in KRAS-wild-type colorectal cancer (CRC) remains unknown. In the present study, functional analysis of overall survival post-diagnosis in patients with KRAS wild-type and those with mutant CRC was performed using human CRC specimens. Furthermore, it was demonstrated that multidrug resistance (MDR) cancer cell-derived exosomes were potentially a key factor, which promoted cetuximab-resistance in CRC cells and reduced the inhibitory effect of cetuximab in CRC xenograft models. The Cell Counting Kit-8 and colony formation assays were performed to assess the effects of exosomes derived from CRC/MDR cells on cetuximab resistance. Sphere formation assay results demonstrated that exosomes derived from CRC/MDR cells altered the self-renewal and multipotential ability of stem-cell-associated markers and facilitated resistance to cetuximab in cetuximab-sensitive cells. Furthermore, exosomes derived from CRC/MDR cells decreased sensitivity to cetuximab via the activation of PI3K/AKT signaling, which promoted Sox2 and programmed death-ligand 1 (PD-L1) mRNA and protein expression according to reverse transcription-quantitative PCR, western blotting and immunohistochemistry analyses, as well as apoptosis resistance both *in vitro* and *in vivo* according to a TUNEL assay. In conclusion, the results of the present study demonstrated that exosomes derived from CRC/MDR cells may promote cetuximab resistance in KRAS wild-type cells via activation of the PI3K/AKT signaling pathway-mediated expression of Sox2 and PD-L1, which will be useful for investigating a potential clinical target in predicting cetuximab resistance.

Correspondence to: Professor Hua Sui, Medical Experiment Center, Jiading Branch of Shanghai General Hospital, Shanghai Jiao Tong University School of Medicine, 800 Huangjiahuayuan Road, Shanghai 201803, P.R. China
E-mail: syh0808@163.com

Professor Huirong Zhu, Department of Medical Oncology, Shuguang Hospital, Shanghai University of Traditional Chinese Medicine, 1200 Cailun Road, Shanghai 201203, P.R. China
E-mail: huirong_zhu@126.com

*Contributed equally

Abbreviations: KRAS, Kirsten rat sarcoma viral oncogene homolog; EGFR, epidermal growth factor receptor; CRC, colorectal cancer; mCRC, metastatic CRC; MDR, multidrug resistance; TCGA, The Cancer Genome Atlas; CSCs, cancer stem cells; TME, tumor microenvironment; L-OHP, oxaliplatin; CCK-8, Cell Counting Kit-8; MAPK, mitogen-activated protein kinase

Key words: exosome, cetuximab, cancer stem cell, resistance, colorectal cancer

Introduction

Colorectal cancer (CRC) is the third most common cancer worldwide and metastatic CRC (mCRC) continues to be associated with a poor prognosis (1). Therapeutic strategies for mCRC have improved over the past decades (2). However, there is an urgent need for novel therapeutic strategies for the patients who exhibit cancer progression even after treatment with cytotoxic chemotherapy and targeted agents (3). KRAS mutation represents one of the most prevalent genetic alterations in cancers (4). In CRC tumors, 85-90% of KRAS mutations occur in exon 2, with codon 12 and 13 being the most predominant

mutations (5). Anti-EGFR antibodies, such as cetuximab or panitumumab, have been demonstrated to be effective against RAS oncogene wild-type mCRC. However, patients will eventually develop drug resistance and further disease progression will occur regardless of the initial efficacy (6).

Therefore, a concentrated research effort has been made to elucidate the mechanism underlying the acquisition of resistance to anti-EGFR therapy by CRC. The occurrence of tumor somatic mutations in the RAS/RAF/MAPK, PI3K/PTEN/AKT and Janus kinase/STAT signaling pathways, have been reported to be potential therapeutic targets in CRC (7). However, therapeutic approaches proposed for overcoming resistance to anti-EGFR therapy have rarely been demonstrated to confer significant clinical benefits (8,9). Increasing evidence indicates that the tumor microenvironment (TME), including tumor-stromal cell interactions, also contributes to changes in tumor characteristics during tumor initiation and progression (10,11). These characteristics of the TME, including helping the formation of cancer stem cells (CSCs), are responsible for the development and maintenance of tumors and resistance to cytotoxic drugs (12).

Furthermore, based on the Hierarchy (CSC) Theory, which suggests CSCs are more likely to generate a tumor, it has been reported that CSCs have a longer life span and a greater ability to self-renew compared with non-stem cells (13). Therefore, it can be hypothesized that alterations in the TME prompt cetuximab resistance in CRC cells and that CSCs may be the intrinsic driving force for activating or inducing cetuximab resistance.

It has previously been demonstrated that certain specific exosomes, which are considered to be the main group of extracellular vesicles, are biologically active lipid-bilayer vesicles that are naturally released from different types of normal or tumor cells (14). Exosomes are lipid bilayer membrane vesicles (50-100 nm) derived from the luminal membrane of multivesicular bodies and are secreted via the fusion of multivesicular bodies with the plasma membrane or via budding from the membrane (15). These vesicles contain nucleic acids, proteins and lipids, which thereby allows for the transfer of genetic material and enable the exchange of information between cells within the microenvironment (10).

Our previous study has demonstrated that exosomes serve a key role in transmitting multidrug resistance (MDR) between tumor cells (16). However, few studies have been reported that the features that contribute to the transmissibility of drug resistance via exosomes in cetuximab-acquired resistant CRC (17). Furthermore, drug resistance often occurs following chemotherapy combined with cetuximab therapy in the clinic (18). Therefore, there is need for further investigations into the mechanism of anti-EGFR therapy resistance to support the development of novel therapeutic strategies.

In the present study, the potential association between exosomes derived from MDR cells and the response to anti-EGFR treatment in CRC cell lines was investigated. Furthermore, the possible effects of exosomes on sensitivity to anti-EGFR treatment were explored *in vivo* and *in vitro*. This suggested that inhibition of the secretion of exosomes from MDR cells could potentially represent a rational therapeutic strategy to prevent and overcome cetuximab resistance in patients with mCRC.

Materials and methods

The Cancer Genome Atlas (TCGA) gene expression data. The TCGA database (https://www.cancer.gov/about-nci/organization/ccg/research/structural-genomics/tcga) created by the National Cancer Institute and the National Human Genome Research Institute, has characterized over 20,000 primary cancer and matched normal samples spanning 33 cancer types worldwide. The TCGA-colon adenocarcinoma study dataset (accession no. phs000178) was chosen to produce a survival curve for CRC. The gene expression profile data (mRNA) of patients with colon cancer were downloaded from TCGA database, and the gene expression profile data was transformed with lg2(x + 1). Samples with missing data and large differences were removed, 372 colon cancer samples were identified, and the expression status of the KRAS gene in patients with colon cancer was analyzed. According to the median KRAS mRNA expression, the samples were divided into the KRAS mutant group and KRAS wild-type group.

Patients and sample collection. A total of 60 patients with CRC patients were enrolled in the study and fresh tissue samples were collected and fixed with 10% formalin solution at 23˚C for 48 h after obtaining written informed consent between January 2020 and January 2022 at Shuguang Hospital, Shanghai University of Traditional Chinese Medicine (Shanghai, China). All patients with CRC were diagnosed according to Chinese Society of Clinical Oncology diagnosis and treatment guidelines for colorectal cancer 2018 (19). The inclusion criteria were as follows: i) Pathologically confirmed colon cancer; ii) stage I to III in TNM pathological staging according to the American Joint Committee on Cancer (20); iii) men or women aged 18-75 years; iv) Karnofsky's performance scoring ≥70 (21); v) no strict heart, liver, kidney or hematopoietic system disease or other factor affecting drug evaluation; and vi) volunteers who had given informed consent. Patients with any of the following conditions were excluded: i) Did not meet the inclusion criteria; ii) mental disorder, pregnancy or lactation; and iii) incomplete information. The patients in the CRC group were aged 45-75 years, with a mean age of 52±11 years. The patients in the advanced CRC group were aged 45-75 years, with a mean age of 54±14 years (Table SI). Among the 18 patients with early-stage CRC (age range, 45-75 years), with a mean age of 52±11 years enrolled in the present study, 8 were male and 10 were female. Of the 32 patients with advanced CRC (the majority of patients were diagnosed in advanced stages, which refers to stage II and III colon cancer) (22,23) (age range, 45-75 years; mean age, 54±14 years), 20 were male and 12 were female. Tumor samples and paired adjacent tissues were collected from all patients. Written informed consent was obtained from every patient.

The present study was approved by the Medical Ethics and Human Clinical Trial Committee of the affiliated hospital, Shuguang Hospital, Shanghai University of Traditional Chinese Medicine (Shanghai, China).

Establishment of the CRC/MDR cell line. The human HCT116, LoVo, Caco-2, HT-29 and SW480 CRC cell lines were purchased from The Cell Bank of Type Culture Collection of

The Chinese Academy of Sciences. The HCT116 and LoVo cells were grown at 37˚C in a 5% CO_2 humidified atmosphere in RPMI 1640 (HyClone; Cytiva) supplemented with 10% (v/v) heat-inactivated fetal calf serum (Gibco; Thermo Fisher Scientific, Inc.), 2 mM glutamine, 100 units/ml penicillin and 100 μg/ml streptomycin (Invitrogen; Thermo Fisher Scientific, Inc.). The HT-29, Caco-2 and SW480 cells were grown at 37˚C in a 5% CO_2 humidified atmosphere in F12K (HyClone; Cytiva), DMEM (HyClone; Cytiva) and L-15 medium (HyClone; Cytiva), respectively, supplemented with 10% (v/v) heat-inactivated fetal calf serum (Gibco; Thermo Fisher Scientific, Inc.), 2 mM glutamine, 100 units/ml penicillin and 100 μg/ml streptomycin (Invitrogen; Thermo Fisher Scientific, Inc.). The HCT116/oxaliplatin (L-OHP) cells were established by gradually increasing the concentration of L-OHP in parental cells (HCT116) first. Subsequently, the cells were intermittently treated with a high-dose concentration (9.6-19.2 μg/ml) of L-OHP (24). Then they were routinely maintained in RPMI 1640 medium containing 5,000 ng/ml L-OHP (Sigma-Aldrich; Merck KGaA) as previously reported (25). The HCT116/L-OHP cells were designated as CRC/MDR cells (Table I) and maintained at 37˚C in a 5% CO_2 humidified atmosphere in the L-OHP-containing medium containing RPMI 1640 supplemented with 10% (v/v) heat-inactivated fetal calf serum (Gibco; Thermo Fisher Scientific, Inc.); 2 mM glutamine, 100 units/ml penicillin and 100 μg/ml streptomycin (Invitrogen; Thermo Fisher Scientific, Inc.), and 5 μg/ml L-OHP (Sigma-Aldrich; Merck KGaA). A cell proliferation analysis assay was performed as described subsequently to detect the IC_{50} values of chemotherapeutic drugs in MDR HCT116/MDR cells and parental HCT116 cells, which were treated with chemotherapeutic drugs with increasing concentrations (0, 125, 250, 500 and 1,000 μg/ml), including VCR, cDDP, 5-Fu and MMC, for 48 h at 37˚C. However, CRC/MDR cells were cultured in L-OHP-free media for 1 week at 37˚C prior to subsequent experimentation to make sure the cells were all in the same environment (26,27). The human CRC Caco-2 and HT-29 cell lines are usually considered as KRAS wild-type (28,29) and were purchased from The Cell Bank of Type Culture Collection of The Chinese Academy of Sciences with a statement of authentication.

Exosome isolation and characterization. The CRC/MDR cells were cultured in exosome-depleted complete medium (Serum-free Media for exosome culture; Umibio) while CRC cells were cultured in normal medium for 48 h at 4˚C. Exosomes were extracted from tumor cells, including CRC and CRC/MDR cells via ultracentrifugation. Briefly, the supernatant was obtained via centrifugation at 2,000 x g for 30 min at 4˚C and 10,000 x g for 30 min at 4˚C as previously reported (30). The medium was then filtered using a 0.22-μm filter, followed by ultracentrifugation at 120,000 x g for 70 min at 4˚C.

The exosome-enriched pellets were suspended in 50 μl PBS. For exosome TEM observation, 5 μl exosomes were loaded onto formvar carbon-coated grids, and were fixed with 1% glutaraldehyde solution at 4˚C overnight. Subsequently, the exosomes were negatively stained with 50 μl 2% aqueous phosphotungstic acid for 60 sec at 23˚C. The exosomes were imaged with a transmission electron microscope at 80 kV. The number and size distribution of the exosomes were detected using a NanoSight LM10 Nanoparticle Characterization System (Malvern Instruments, Inc.). The exosomal protein concentration was quantified via the BCA method and exosome-associated protein marker HSP70 and CD81 expression was analyzed via western blotting.

Table I. Sensitivity to chemotherapy in HCT116 and HCT116/MDR cells.

Chemotherapeutic drugs	IC_{50} (μg/ml)		Resistance factor
	HCT116	HCT116/MDR	
L-OHP	19.84±1.42	157.48±16.73[a]	7.94
cDDP	3.32±0.37	26.38±1.92[a]	7.95
5-Fu	7.14±1.21	33.29±3.64[a]	4.66
MMC	2.55±0.35	12.50±2.49[a]	4.90

[a]P<0.01 vs. HCT116. MDR, multidrug resistance; L-OHP, oxaliplatin; cDPP, cisplatin; 5-Fu, fluorouracil; MMC, mitomycin C.

Western blotting. Tumor cell (HT-29 and Caco-2 cells) proteins were extracted using RIPA lysis buffer (Beyotime Institute of Biotechnology) as previously reported (31). Protein concentration was quantified using the BCA method. A total of 40 μg protein for each group was separated via SDS-PAGE on a 12% gel and transferred to 0.45 μm PVDF membranes (Merck KGaA). Membranes were blocked with 5% BSA (Beyotime Institute of Biotechnology) for 2 h at 23˚C and then incubated with primary antibodies against the following proteins at 4˚C overnight: HSP70 (1:1,000; cat. no. 4876; Cell Signaling Technology, Inc.), CD81 (1:1,000; cat. no. ab79559; Abcam), EGFR (1:1,000; cat. no. 66455; ProteinTech Group, Inc.), phosphorylated (p)-EGFR (1:1,000; cat. no. 18986; ProteinTech Group, Inc.), AKT (1:1,000; cat. no. 4691; Cell Signaling Technology, Inc.), p-AKT (1:1,000; cat. no. 13038; Cell Signaling Technology, Inc.), Sox2 (1:1,000; cat. no. 3579; Cell Signaling Technology, Inc.) and programmed death-ligand 1 (PD-L1; 1:1,000; cat. no. 66248; ProteinTech Group, Inc.). GAPDH rabbit monoclonal antibody (1:1,000; cat. no. 5174; Cell Signaling Technology, Inc.) and tubulin rabbit monoclonal antibody (1:1,000; cat. no. 2148; Cell Signaling Technology, Inc.) were used as the internal control. The membranes were washed three times with TBS with 0.1% Tween-20 (TBST) and incubated at 37˚C for 1 h with HRP-conjugated anti-rabbit secondary antibody (1:2,000; cat. no. ab97051; Abcam) and HRP-conjugated anti-mouse secondary antibody (1:2,000; cat. no. ab6728; Abcam). Then, the membranes were washed three times with TBST. Bands were visualized via chemiluminescence using Immobilon® ECL Ultra Western HRP Substrate (Merck KGaA) according to the manufacturer's protocol and a ChemiScope 6200 Touch (Clinx Science Instruments Co., Ltd.). The data were analyzed using ImageJ software (version 1.8.0; National Institutes of Health).

Sphere formation assay. The cells were transferred to ultra-low attachment plates (Corning, Inc.) in serum-free DMEM

(HyClone; Cytiva) containing 10 ng/ml Fibroblast Growth Factor (basic) (FUJIFILM Wako Pure Chemical Corporation), 10 mg/ml human insulin (CSTI), 100 mg/ml human transferrin (Roche Diagnostics) and 100 mg/ml BSA (Nacalai Tesque, Inc.) and incubated at 37˚C in a 5% CO_2 incubator for 10 days. The number of cell spheres, defined as spherical, non-adherent cell clusters <100 μm in diameter, was quantified and the spheres were imaged using an inverted light microscope and analysed using ImageJ software (version 1.8.0; National Institutes of Health).

Reverse transcription-quantitative PCR (RT-qPCR). RNA was extracted from HT-29 and Caco-2 cells ($1x10^6$) using TRIzol® (Takara Bio, Inc.) as previously reported (25). Total RNA was reverse transcribed into complementary DNA using the SuperScript™ IV First-Strand Synthesis System (Thermo Fisher Scientific, Inc.) according to the manufacturer's instructions. Then, the mixture system, including SYBR Green qPCR Master mix (Thermo Fisher Scientific, Inc.), cDNA templates and primers were applied for qPCR to detect the mRNA expression according to the manufacturer's instructions. The thermocycling conditions were: 95˚C for 3 min, followed by 40 cycles of 95˚C for 15 sec and 60˚C for 15 sec. Primer sequences for target genes, CD133, Nanog, Oct-4, CD29, CD44, Sox2 and GAPDH are presented in Table SII. GAPDH was used as the reference gene. The mRNA expression levels were quantified using the CFX Connect Real-Time PCR Detection System (Bio-Rad Laboratories, Inc.) and were analyzed using the CFX management software v2.0 (Bio-Rad Laboratories, Inc.). Relative quantification of mRNA was performed using the $2^{-\Delta\Delta Cq}$ method (32).

Cell proliferation analysis. HT-29 and Caco-2 cells were seeded into 96-well plates (5,000 cells/well) and exposed to increasing concentrations of cetuximab (0, 125, 250, 500 and 1,000 μg/ml; Merck & Co., Inc.) for 24, 48 and 72 h at 37˚C. The proliferative ability of cells was determined using the Cell Counting Kit-8 (CCK-8; Med Chem Express) assay for 2 h according to the manufacturer's protocol and is presented as cell proliferation (%). Absorbance was quantified at 450 nm using a Cytation 5 Cell Imaging Multi-Mode Reader (BioTek Instruments, Inc.). The half-maximal inhibitory concentration (IC_{50}) of drugs was determined using GraphPad Prism version 8.0 (GraphPad Software, Inc.).

Colony formation assays. The HT-29 and Caco-2 cells were seeded in six-well plates (~100 cells/well). Cells were treated with different exosomes for 72 h as previously reported (33). Subsequently, cells were washed twice with PBS, cultured in RPM1640 medium and DMEM (HyClone; Cytiva) and allowed to form colonies at 37˚C for 14 days. Media were replaced every 4-5 days. Cell colonies were defined as cell populations >0.5 mm in diameter and the number of cell colonies was counted manually. Colonies were washed three times with PBS, and were then fixed with 95% ethanol at room temperature for 20 min. Colonies were stained with crystal violet (2%) at 37˚C for 30 min. Following extensive washing with PBS, the cells were observed under a light microscope (Olympus Soft Imaging Solutions GmbH) and five fields were selected randomly for colony counting. The colony formation rate was then calculated using the following equation: Colony formation rate=(number of clones)/(number of seeded cells) x100%.

Sphere formation assay for tumor stem cells. For formation of spheres, cells were cultured in NeuroCult NS-A basal serum-free medium (human; Stemcell Technologies, Inc.) supplemented with 20 μg/ml heparin (Stemcell Technologies, Inc.), 20 ng/ml hEGF (R&D Systems, Inc.), 10 ng/ml hFGF-b (PeproTech, Inc.) and NeuroCult NS-A Proliferation Supplements (Stemcell Technologies, Inc.). This combination of medium is usually used for stem cells. Cells were seeded at low densities in 12-well low-adhesion plates (1 ml per well). The cells were cultured and then seeded at clonal density in low-adhesion plates. The spheroids were grown until Day 7 and images were captured at a magnification of x100 using an inverted light microscope (first-generation). Thereafter, the first-generation spheroids were dissociated to single cells, and equal numbers of live cells were cultured. Subsequently, the cells were plated at clonal density, resulting in second-generation spheroids. The number of second-generation spheroids was quantified using ImageJ software (version 1.8.0; National Institutes of Health). As previously reported, 7 days were considered to be one cycle (34). Viable spheres were those active spheres which had the ability to grow just like cells. These viable spheres defined as SP cells possessing stem cell characteristics, such as proliferation, self-renewal and differentiation (35).

Tumor mouse model. HT-29 cells were harvested in serum-free PBS and 100 μl cell suspensions ($1x10^7$ cells/ml) were injected subcutaneously into 20 female BALB/c nude mice (age, 6-8 weeks; weight, ~20.0±0.6 g; Shanghai SLAC Laboratory Animal Co. Ltd.; license no. SCXK2017-0005). The animal experiment was approved by the Institutional Animal Care and Use Committee of Shuguang Hospital, Shanghai University of Traditional Chinese Medicine (approval no. PZSHUTCM200 724027). The animals were kept under specific pathogen-free conditions. The room temperature was 20˚C, the relative humidity was 60%. The light/dark cycle was 12/12 h. The animals had free access to drinking water and food normally, and were fasting for 12 h before the experiment. When the tumors reached an average volume of 100 mm^3, the mice were randomly divided into four groups (n=5) as follows: i) Saline (0.2 ml per mouse) intraperitoneal injection daily; ii) 0.05 g/kg cetuximab solution intraperitoneal injection every other day; iii) 100 μl CRC exosomes peritumoral injection then 0.05 g/kg cetuximab solution intraperitoneal injection every other day; iv) 100 μl CRC/MDR exosomes peritumoral injection then 0.05 g/kg cetuximab solution intraperitoneal injection every other day. The length and width of tumors were recorded every 3 days. After 27 days from the first day as marked as day 0, according to the Guideline of assessment for humane endpoints in animal experiment (RB/T 173-2018), the diameter of tumors was <1.2 cm. The humane endpoints in the present study were that the animals showed no activity, including grooming, food intake of <1 g per day, or >20% body weight loss over 3 days (the maximum body weight loss over the entire experimental period was <15% and the maximum body weight loss over 3 days was <12%), or the diameter of tumors was >1.2 cm. The

animals were sacrificed via cervical dislocation in deep anesthesia (5% isoflurane; 5 l/min for 1 min) and were surgically removed primary tumors and weighed. Tumor volumes were quantified using the following formula: length x width^2 x 0.5.

TUNEL assay. The TUNEL assay was performed using a DeadEnd™ Colorimetric TUNEL System kit (Promega Corporation) to detect the apoptosis of the subcutaneous tumors according to the manufacturer's protocol (16). The peeled tumor was washed with xylene twice for 5 min each. The tumors were fixed with 10% neutral formalin at 23˚C for 3 h, dehydrated in gradient alcohol, embedded in paraffin, and sliced into 4-μm thick slices, and heated at 65˚C for 1 h. The tissues were dewaxed, washed with running water and repaired with pH 8.0 EDTA antigen repair solution in a water bath at 98˚C for 25 min. The tissue was treated with Proteinase K working liquid for 15-30 min, and the mixture of the TUNEL reaction was prepared according to the instructions. TUNEL working solution was added to the tissues and these were incubated in the dark at 37˚C for 60 min. The samples were rinsed with PBS three times. Subsequently, 50 μl converter-POD was added to the specimen after the slide was dried. The slide was covered and reacted at 37˚C in a dark wet box, and rinsed three times within 30 min. Subsequently, 50 μl 5 mg/ml DAPI substrate was added and tissues were incubated at 25˚C for 3 min. The tissues were rinsed with PBS for 10 min at 25˚C. Subsequently, the tissue was sealed with Anti-Fade Mounting Medium (ab104135; Abcam). A drop of glycerin was added to observe the apoptotic cells (200-500 cells in total) and capture images with a 20x objective and 10x eyepiece. Three random fields of view per sample were observed. The observation and capture of digital images was performed using a Nikon E80i fluorescence microscope (Nikon Corporation).

Immunohistochemistry (IHC). Tumor tissue samples were fixed with 4% paraformaldehyde solution for 3 h at 23˚C, and then embedded with paraffin after gradient dehydration. Paraffin-embedded tumor tissue samples (5-μm-thick sections) were selected for IHC. Slices were placed in an oven for 30 min for dewaxing and were then hydrated with gradient alcohol. Subsequently, the slides were washed again with PBS and incubated with the prefabricated avidin peroxidase macromolecular complex for 30 min. The peroxidase reaction was completed by incubation in PBS containing 0.01% hydrogen peroxide at room temperature for ~5 min. The paraffin sections were incubated in the sealing solution [10% donkey serum (Gibco; Thermo Fisher Scientific, Inc.) + 5% skim milk + 4% BSA + 0.1% TritonX-100] for 10 min, then incubated with antibodies at 4˚C overnight. The primary antibodies for IHC were p-EGFR (1:750; cat. no. 18986; ProteinTech Group, Inc.), p-AKT (1:300; cat. no. 4060; Cell Signaling Technology, Inc.), Sox2 (1:300; cat. no. 14962; Cell Signaling Technology, Inc.) and PD-L1 (1:300; cat. no. 66248; ProteinTech Group, Inc.). The slides were washed again with PBS. The slices were incubated with Polymer helper for 20 min, and then washed with PBS for 5 min three times. Subsequently, the samples were incubated with an HRP-conjugated goat anti-rabbit IgG secondary antibody (1:2,000; cat. no. ab6702; Abcam) at 37˚C for 1 h. DAB (cat. no. ab64238; Abcam) was added immediately after the liquid around the tissue dried, slides were incubated at room temperature for 10 min and the reaction was terminated with water washing. The slices were dehydrated and made transparent after counter-staining with hematoxylin for 5 min at room temperature. Results of staining were assessed using a Nikon E80i light microscope (Nikon Corporation).

Statistical analysis. SPSS version 21.0 (IBM Corp.) was used for the statistical analysis. DFS was compared using a two-sided log-rank test. Hazard ratios with 95% confidence intervals were calculated using the Cox proportional hazards model. The Kaplan-Meier method was used to draw survival curves, and a log-rank test was carried out to compare the survival rates. The Wilcoxon test was used for continuous variables and Pearson's χ^2 test for categorical variables. All data obtained in the present study are presented as the mean ± SD from at least three independent experiments. Statistical analyses were performed using GraphPad Prism 8.0 (GraphPad Software, Inc.). A two-sided unpaired Student's t-test with Benjamini-Hochberg correction was used to compare two groups. Differences among three or more groups were analyzed using one-way ANOVA followed by Tukey's post-hoc test. $P<0.05$ was considered to indicate a statistically significant difference.

Results

Activation of the EGFR signaling pathway is associated with a poor prognosis in cetuximab-treated patients with CRC. According to IHC scoring (36) results, 78.3% (47/60) and 20.0% (12/60) of tumors were defined as presenting high and low BRAF protein expression levels, respectively (Fig. 1A). Analysis of the TCGA gene expression data demonstrated that the overall survival rate at 3 years postdiagnosis in patients with KRAS wild-type (n=229) was markedly higher than the overall survival rate in patients with the KRAS mutation (n=143) ($P<0.05$). However, 3-12 years postdiagnosis, the overall survival rates in patients with KRAS wild-type were lower than overall survival rates in patients with the KRAS mutation (Fig. 1B). As previously reported, KRAS-mutant CRC is associated with a poorer prognosis compared with KRAS wild-type CRC (37).

The dose and time-dependent effects of cetuximab on cell proliferation were assessed using the CCK-8 assay to explore the sensitivity of different CRC cell lines to cetuximab. Caco-2 and HT-29 cell lines with cetuximab treatment exhibited a marked cetuximab-sensitive phenotype compared with the other CRC cell lines (HCT116, HCT116/L, LoVo and SW480 cells) (Fig. 1C). It should be noted that although the cell proliferation was slightly increased at 72 h compared with 48 h in HT-29 cells, the difference was too small to be statistically significant. Anti-EGFR antibody treatment was effective in the KRAS wild-type Caco-2 and HT-29 cell lines, which were used as cetuximab-sensitive cells in the subsequent experiments.

Exosomes derived from CRC/MDR cells could increase resistance to cetuximab in vitro. Increasing evidence suggests that exosomes secreted by cancer cells are key mediators of cell-to-cell communication (16,38) and have the capacity to considerably modify the TME, which impacts disease

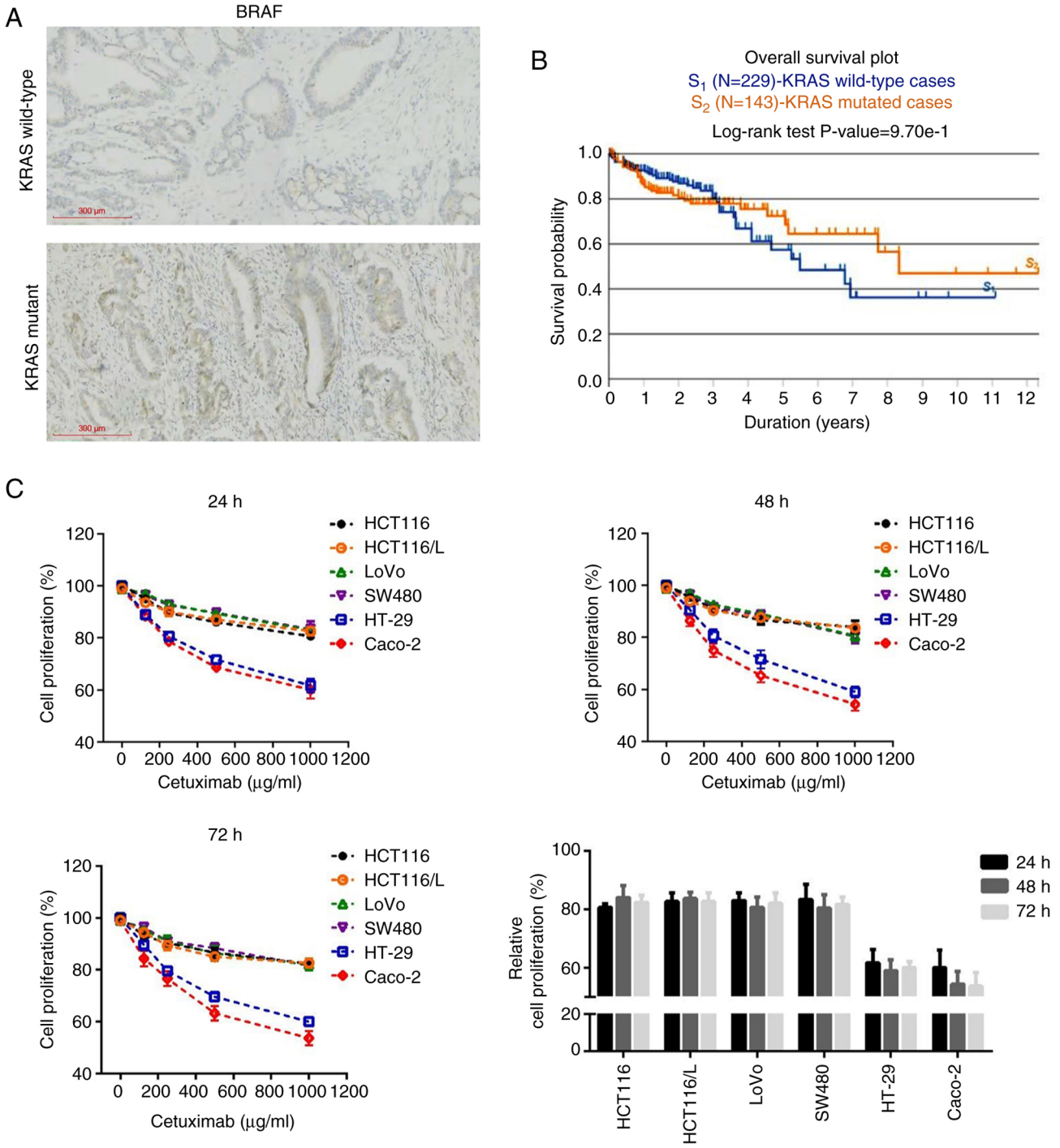

Figure 1. EGFR signaling pathway is associated with poor prognosis in patients with KRAS mutation with colorectal cancer. (A) Immunohistochemistry scoring criteria to classify tumor BRAF protein expression. Representative immunohistochemistry micrographs of KRAS in KRAS mutation and KRAS wild-type tissue. Scale bar, 300 μm. (B) Kaplan-Meier plot showing the overall survival probability of patients with metastatic colorectal cancer according to genetic profile (KRAS mutation vs. KRAS wild-type). (C) Cells were cultured with 0, 125, 250, 500 or 1,000 μg/ml cetuximab for 24, 48 and 72 h. A Cell Counting Kit-8 assay was used to assess relative cell proliferation of CRC cells in relation to controls, which were not treated with cetuximab.

progression. Compared with HCT116 cells, HCT116/MDR cells showed chemotherapeutic drug resistance (Table I), and the difference was statistically significant (P<0.01). The exosomes secreted from CRC/MDR cells and their parental sensitive CRC cells were analyzed for their phenotype (purity and shape) using TEM and for size and particle number using the LM10 Nanoparticle Characterization System (Fig. 2A). A previous study reported that the particles were determined to be cup-shaped membrane-bound vesicles with a diameter of ~100 nm (39). The mean diameter of these nanovesicles ranged between 90 and 120 nm for exosomes from both CRC/MDR cells and their parental sensitive CRC cells (data not shown), which was consistent with the characteristic features of exosomes.

The results of the present study also revealed that the mean sizes of exosomes from CRC/MDR cells and their parental

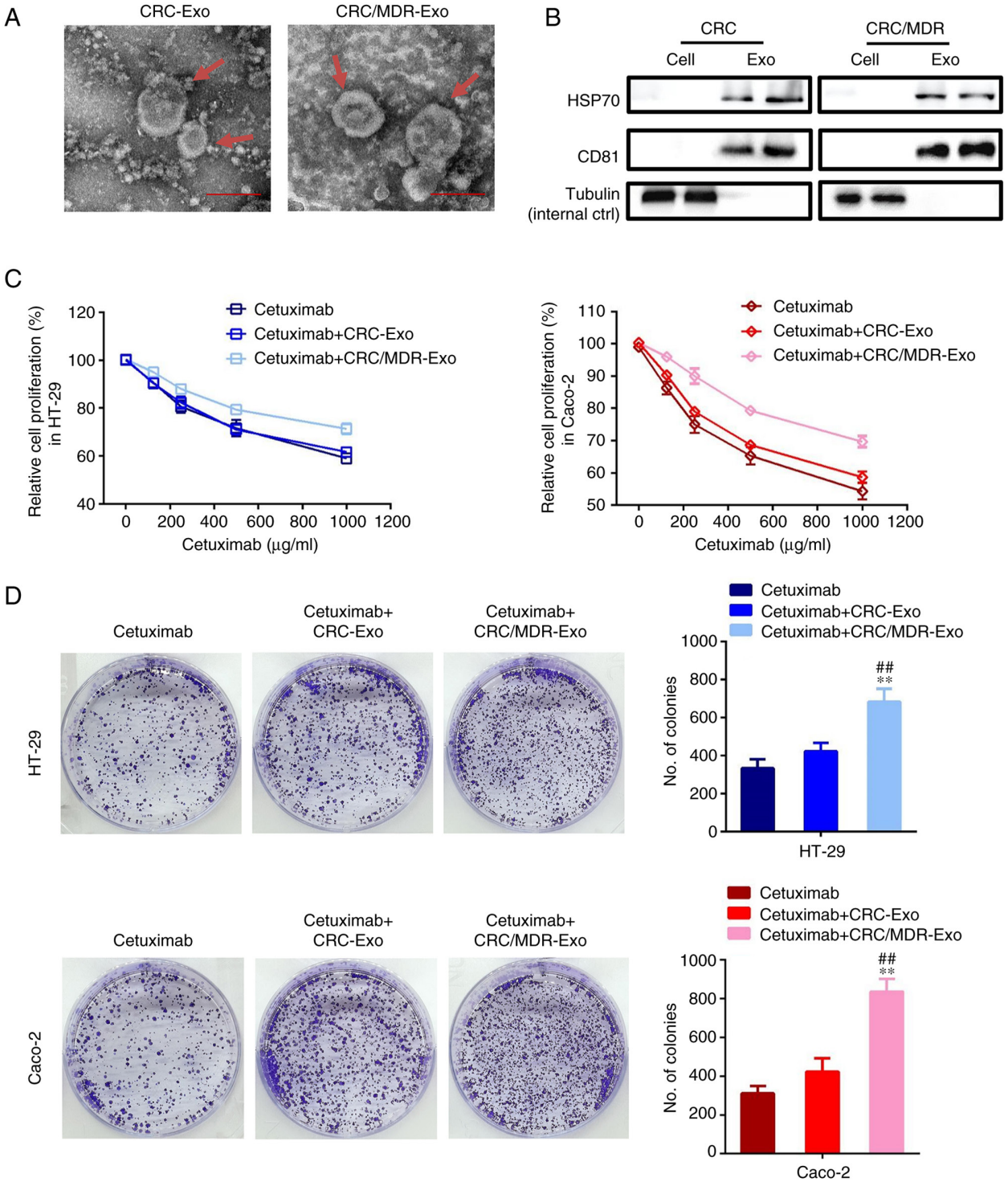

Figure 2. Exosomes derived from CRC/MDR cells increase cetuximab resistance in cetuximab-sensitive cells. (A) Exosomes isolated from the cell culture medium of CRC and CRC/MDR cells were analyzed for phenotype (purity and shape) using TEM. Red arrows indicate representative exosome examples. Scale bar, 100 nm. (B) Western blotting was performed to detect the exosome markers, HSP70 and CD81. Tubulin was used as an internal control. The surface markers of exosomes could not be observed in normal cells. By contrast, tubulin can be observed in cells, while HSP70 and CD81 cannot be observed in cells. (C) A Cell Counting Kit-8 assay was used to assess the effect of cetuximab on the proliferation of HT-29 and Caco-2 cells pre-treated with exosomes derived from CRC/MDR cells or CRC/MDR cells for 72 h in relation to controls, which were not treated with exosomes. The concentrations of cetuximab used for the drug dose-response curve analysis of the indicated cells were 0, 125, 250, 500 and 1,000 μg/ml. (D) HT-29 and Caco-2 cells were treated with exosomes derived from CRC cells and CRC/MDR cells for colony formation analysis. Cells were imaged using a light microscope fitted with a digital camera. The differences among the several groups were analyzed using one-way ANOVA followed by Duncan's test. Data are presented as the mean ± SD from at least three experiments. **P<0.01 vs. cetuximab; $^{\#\#}$P<0.01 vs. cetuximab + CRC-Exo. CRC, colorectal cancer; exo, exosome; MDR, multidrug resistance.

sensitive cells were all between 100 and 200 nm, whereas the particle numbers for the exosomes were all >2.0x10^7 particles/ml (data not shown), although without significant differences. Furthermore, the exosome markers HSP70 and CD81 were detected via western blotting. The exosomes from both CRC/MDR cells and their parental sensitive CRC cells

(referred to as CRC/MDR-Exo and CRC Exo), showed the typical exosomal marker proteins (40) of HSP70 and CD81 (Fig. 2B).

The effect of the exosomes of CRC/MDR cells on the spread of drug resistance of cetuximab to KRAS-wild-type cell lines was investigated. HT-29 and Caco-2 cells were incubated with CRC-exosomes or CRC/MDR-exosomes and treated with cetuximab at different concentrations for cell proliferation analysis. CRC/MDR-exosome treatment markedly reduced the sensitivity of HT-29 and Caco-2 cells to cetuximab (Fig. 2C). Similar efficiency was also noted in the clone formation assay of HT-29 and Caco-2 cells. The clone formation assay showed that compared with the cetuximab group, the CRC-exosome treatment group exhibited no significant differences in colony numbers in HT-29 cells or Caco-2 cells, while the colony formation numbers of both cell lines in the CRC/MDR-exosome group were increased compared with those in the cetuximab group (Figs. 2D and S1).

Exosomes derived from CRC/MDR cells regulate the protein expression levels of EGFR-associated proteins in HT-29 and Caco-2 cells. As demonstrated in a previous study (41), the RAS-RAF signaling pathway is one of the downstream signaling pathways of EGFR, and even if the KRAS gene is mutated in the RAS-RAF signaling pathway, the phenomenon of targeted resistance is not entirely due to the expression of EGFR and p-EGFR. The western blotting results showed that, compared with the control group, the intervention of CRC-exosomes had no significant effect on the expression of EGFR, p-EGFR and Akt in Caco-2 and HT-29 cells (Fig. 3A, C and D). However, the CRC/MDR-exosome intervention had significant effect on the expression of Sox2 and PD-L1 in Caco-2 cells (Fig. 3D).

The phosphorylation levels of AKT were significantly elevated in the CRC/MDR-exosomes group compared with the CRC-exosomes group in HT-29 cells. However, CRC/MDR-exosome treatment demonstrated no significant effect on the phosphorylation levels of AKT in Caco-2 cells (Fig. S2). Therefore, HT-29 cells were selected for subcutaneous xenograft in the animal model.

Based on the aforementioned results and other studies (16,42), we hypothesized that CRC/MDR-exosomes could activate the phosphorylation of components of the PI3K/AKT signaling pathway in HT-29 cells and regulate the Sox2-mediated activity of stem cells in Caco-2 cells. These effects together potentially directed the inhibitory effect of cetuximab resistance in KRAS wild-type cells (Fig. 3B). Furthermore, the present study demonstrated that CRC/MDR-exosomes significantly regulated the protein expression levels of the key EGFR signaling pathway protein AKT in KRAS-wild type cells compared with that in the CRC exosome treatment group.

Exosomes derived from CRC/MDR cells increase tumorigenesis-associated CSC gene expression. Cell proliferation is a fundamental step in tumorigenesis progression, which can be analyzed via sphere-formation. In the present study, the number and size of spheres were quantified and analyzed using stem cell medium to test sphere-forming capacity (Fig. 4A and B). Previous studies reported that a clear distinction could be observed in the capacity of cells to form spheres under different treatment conditions (43,44). Consistent with previous studies, spheres were counted as 10-100 μM size range, and in this size range the spheres had more capability to grow. The present study demonstrated that CRC/MDR-exosomes caused an increase of heterogeneous cell populations containing a number of sphere-forming subpopulations in HT-29 cells and Caco-2 cells compared with the cells without exosomes treatment, especially in the range of 20 to 39, 40 to 59, and 80 to 100 μM size compared with the control group under the same culture conditions. Furthermore, the present study compared the mRNA expression levels of stem-cell-associated markers, such as CD133, Nanog, Oct-4, CD29, CD44 and Sox2, via RT-qPCR to assess whether the spheres formed had the features of tumor-initiating cells. Results of the present study also showed that higher expression levels of Nanog, CD44 and Sox2 were observed under CRC/MDR-exosomes treatment as compared with the normal culture condition without exosome treatment. The expression levels of CD29 were also significantly higher in CRC/MDR-exosome treatment cells compared with cells without exosome treatment in HT-29 cells (Fig. 4C and D). The aforementioned results suggested that sphere forming cells may exhibit increased stemness following treatment with CRC/MDR-exosomes.

Effects of exosomes derived from CRC/MDR cells in vivo. Subcutaneous xenograft of HT-29 cells in nude mouse models was performed to assess whether CRC/MDR-exosomes inhibited the anti-tumor effects of cetuximab *in vivo*. Treatment with exosomes derived from CRC/MDR cells also reduced the inhibitory effect of cetuximab on the tumor growth as compared with cetuximab alone, whereas the exosomes derived from CRC cells greatly recovered the inhibitory effect of cetuximab on the tumor growth (Fig. 5A). Final tumor volume and weight assessment demonstrated that tumors derived from the cetuximab + CRC/MDR-exosomes group were significantly heavier than those in the group of exosomes derived from CRC cells with cetuximab treatment (Fig. 5B and C).

Subsequently, the TUNEL assay was performed to observe the apoptotic tumor cells in the subcutaneous xenograft of HT-29 cells with different treatments (Fig. 5D and E). The treatment of cells with exosomes derived from CRC/MDR cells followed by incubation with cetuximab demonstrated significantly fewer apoptotic tumor cells in the xenograft tumor compared with the cetuximab + CRC-exosome group. However, the TUNEL assay showed the most apoptotic tumor cells in the cetuximab alone group.

Effects of CRC/MDR-exosomes on the protein expression levels of EGFR-associated proteins in vivo. The protein expression levels of p-EGFR, p-AKT, Sox2 and PD-L1 in the xenograft tumor tissues were detected via IHC. The images obtained via IHC demonstrated that treatment with exosomes derived from CRC-MDR cells followed by incubation with cetuximab demonstrated higher expression levels (based on the trend of brown staining in each group) of Sox2 and PD-L1 in the xenograft tumor compared with cetuximab alone. This suggested that exosomes from CRC/MDR cells activated cetuximab-sensitive cells and enhanced cell stemness

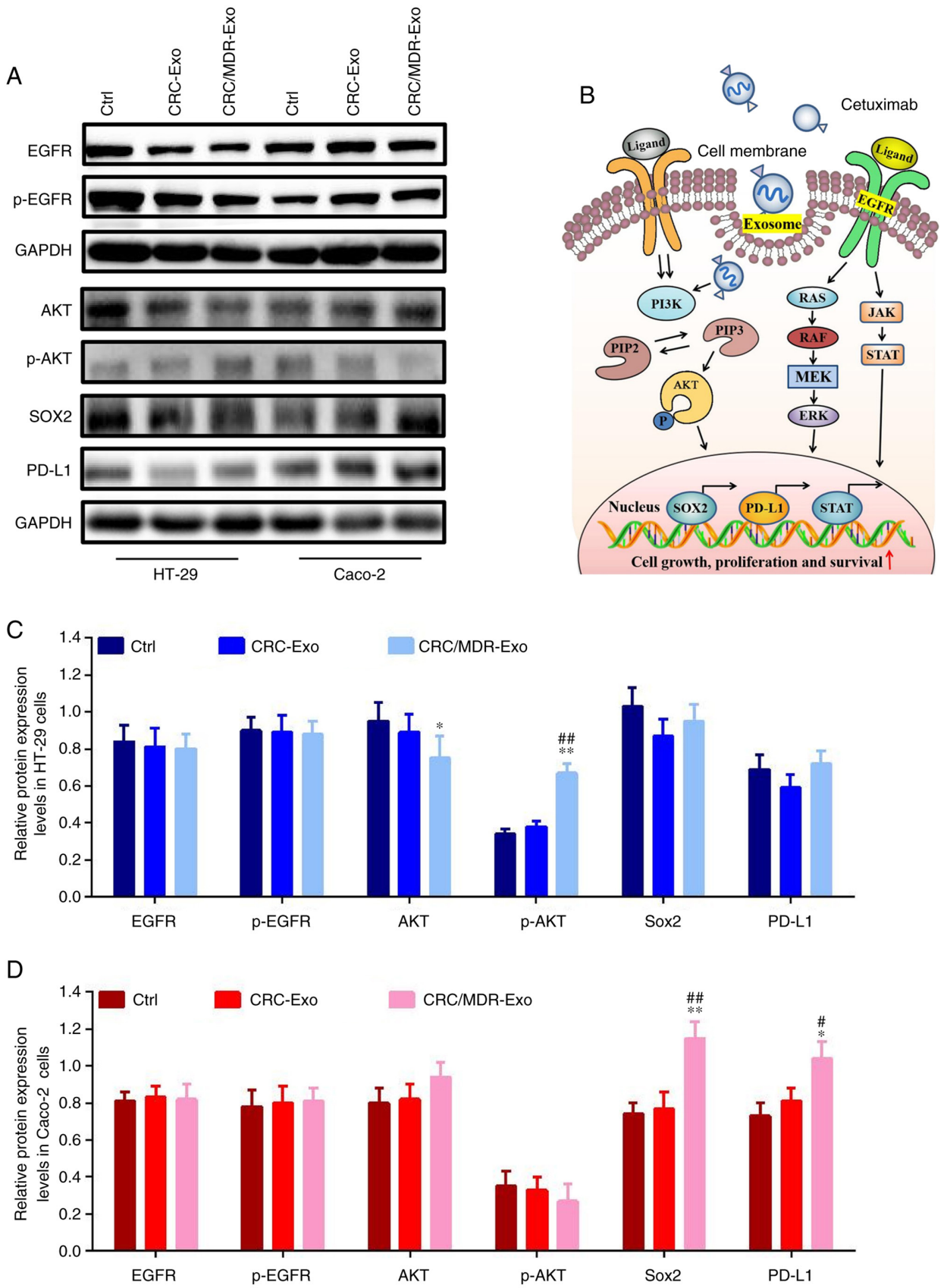

Figure 3. Exosomes derived from CRC/MDR cells regulate EGFR-related protein expression levels in HT-29 and Caco-2 cells. (A) Western blotting of EGFR, p-EGFR, AKT, p-AKT, Sox2 and PD-L1 proteins in HT-29 and Caco-2 cells with the indicated treatments. (B) Proposed working model. In KRAS wild-type CRC cells, the activation of the PI3K/AKT signaling pathway increased cell proliferation and survival, increased the expression and transcription of Sox2 and PD-L1 and resulted in cetuximab resistance. Western blotting quantitative assays of EGFR, p-EGFR, AKT, p-AKT, Sox2 and PD-L1 proteins in (C) HT-29 and (D) Caco-2 cells with the indicated treatments. The differences among the several groups were analyzed using one-way ANOVA followed by Duncan's test. Data are presented as the mean ± SD from at least three experiments. *P<0.05 and **P<0.01 vs. cetuximab; $^{\#}$P<0.05 and $^{\#\#}$P<0.01 vs. cetuximab + CRC-Exo. CRC, colorectal cancer; exo, exosome; MDR, multidrug resistance; Ctrl, Control; p, phosphorylated; PIP2, phosphatidylinositol-4, 5-bisphosphate; PIP3, phosphatidylinositol-3,4,5-triphosphate; JAK, Janus kinase; PD-L1, programmed death-ligand 1.

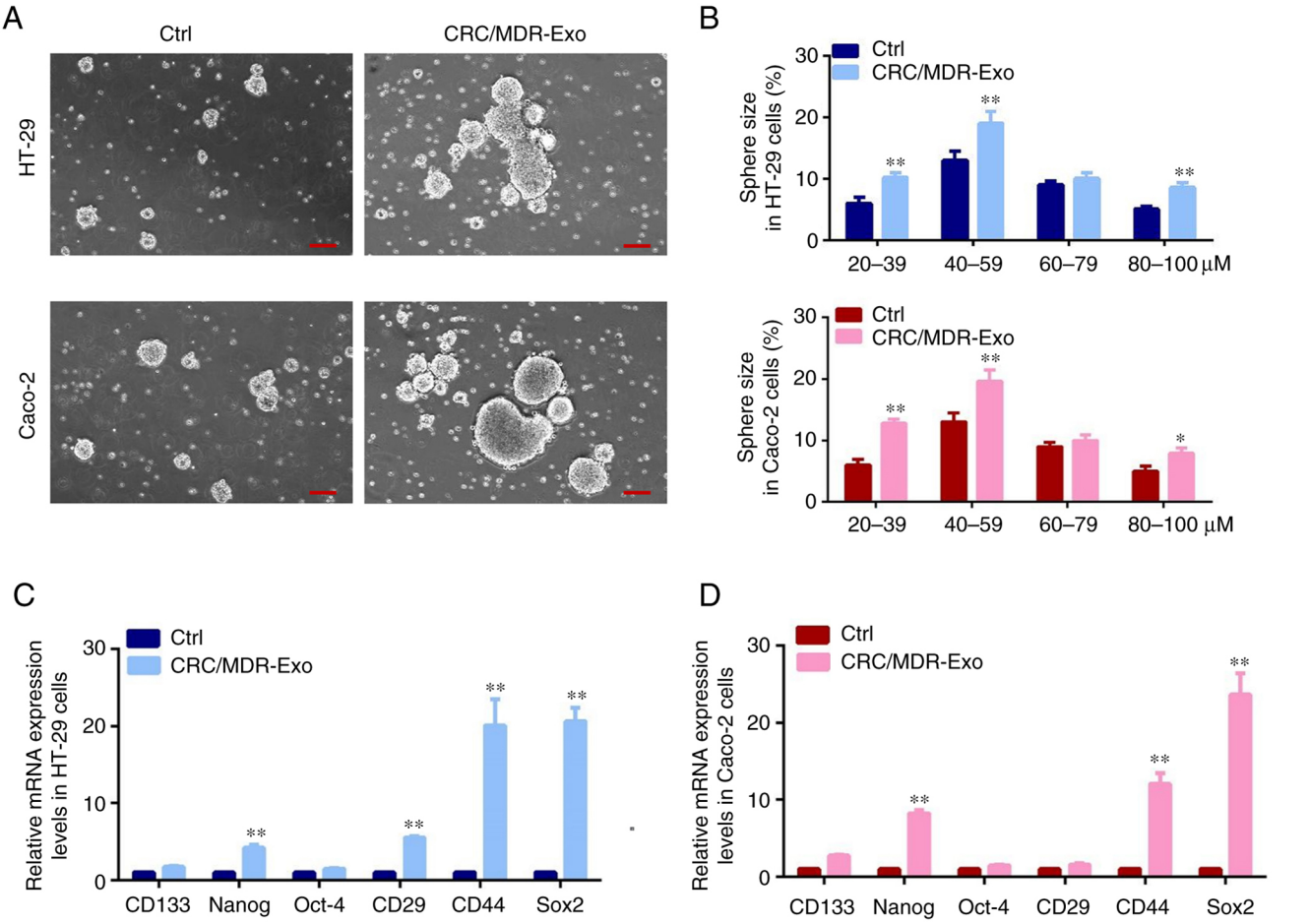

Figure 4. Exosomes derived from CRC/MDR cells increase the population of cetuximab-sensitive cells and stem cell-related gene expression. (A) Representative phase contrast micrographs of cell spheres (diameter ≥200 μm was considered as a sphere) isolated from HT-29 and Caco-2 cells with or without CRC/MDR-exosome treatment. Scale bar, 100 μm. (B) Number and size of spheres were quantified 3 days after plating by counting viable spheres/well. (C and D) mRNA expression levels of CD133, Nanog, Oct-4, CD29, CD44 and Sox2 in HT-29 and Caco-2 cells with or without CRC/MDR-exosome treatment were analyzed via reverse transcription-quantitative PCR. Cells were cultured with normal medium in Control group. The differences among the several groups were analyzed using one-way analysis of variance (ANOVA) followed by Duncan's test. Data are presented as the mean ± SD from at least three experiments. *P<0.05 and **P<0.01 vs. Ctrl. CRC, colorectal cancer; exo, exosome; MDR, multidrug resistance; Ctrl, control.

via stimulation of the PI3k/AKT signaling pathway, which conferred cetuximab resistance in CRC cells (Fig. 6 and Table SIV).

Discussion

Cetuximab is one of the most widely used EGFR inhibitors in the treatment of patients with mCRC and wild-type KRAS status and use in combination with chemotherapy is a standard first-line treatment regimen (8). However, primary or acquired resistance to cetuximab often occurs during targeted therapy (45). To optimize individualized cetuximab therapy in patients with CRC, it is essential to identify the possible mechanism of the response to cetuximab therapy. Previous studies of drug resistance to EGFR inhibitors have focused on understanding resistance mechanisms to EGFR kinase inhibitors and the findings from those studies have been applied to develop the next generation of clinical trials for CRC treatment (41,46). However, there has been limited exploration of the mechanisms of acquired cetuximab resistance and the mechanism of acquired cetuximab resistance has been neglected in the TME.

The TME originates from the idea of 'seed and soil', which was proposed by Stephen Paget (47). The 'seed and soil' hypothesis holds that metastasis depends on the interaction between the 'seed' (cancer cell) and the 'soil' (host microenvironment). Accumulating evidence has demonstrated that exosomes support the development of drug resistance in cancer cells via the secretion of different proteins and nucleic acids in the TME, which can establish drug resistance in nearby or distant cancer cells (10,29,48). It was therefore hypothesized that one mechanism by which MDR cells containing exosomes might facilitate tumor niche development is via the alteration of the tumor stroma. Therefore, the present study aimed to investigate the potential regulatory effect of MDR cells on CRC cells that were sensitive to cetuximab.

TCGA analysis demonstrated that patients with KRAS wild-type had longer progression-free survival than those with KRAS-mutant. Previous data have shown that mCRC lesions harboring KRAS and BRAF mutations are highly associated with a poor prognosis and poor objective response to cetuximab therapy (49). Furthermore, an increasing trend (brown staining indicating positive cells) of serine/threonine-protein kinase BRAF protein expression levels was also identified

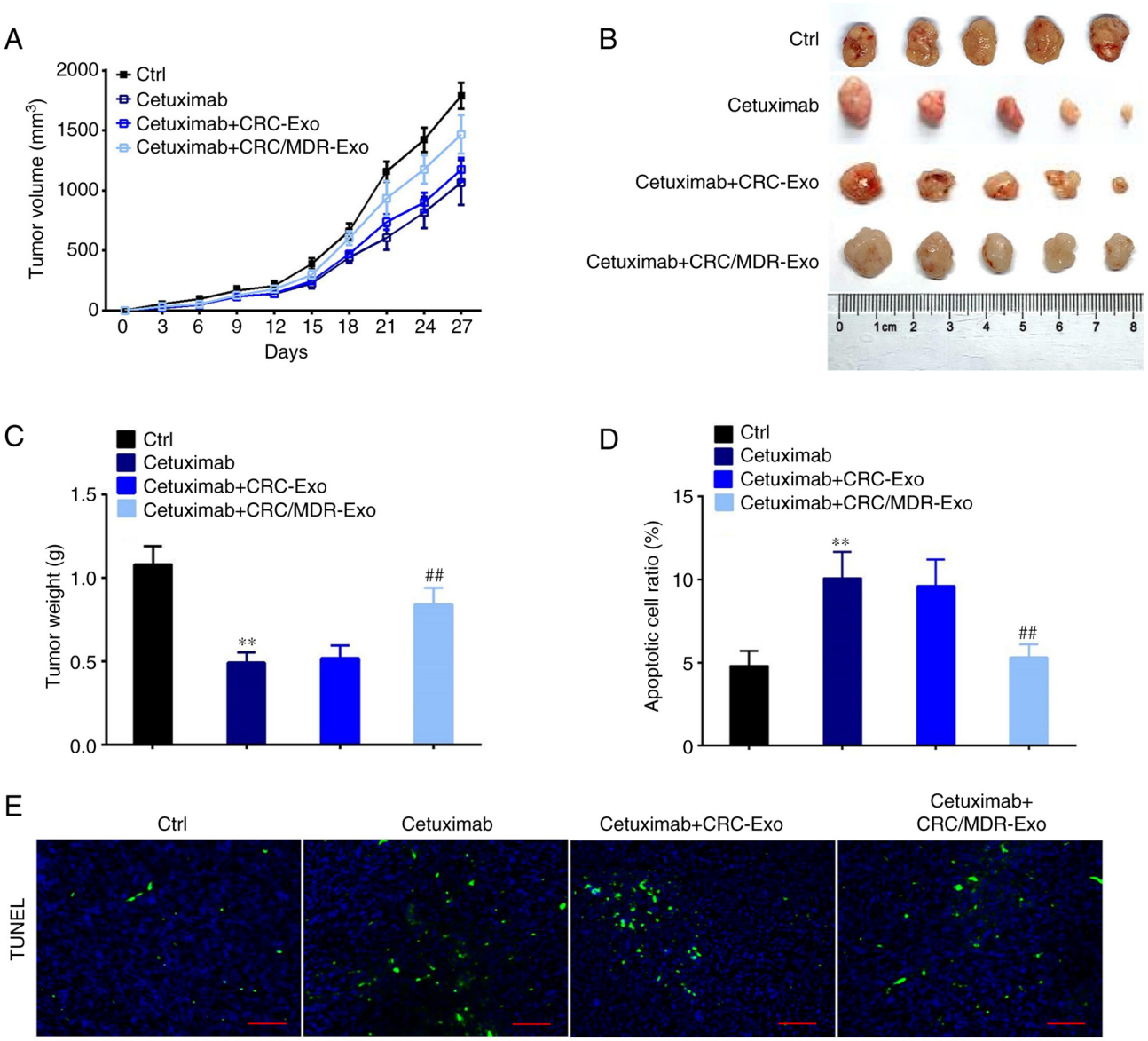

Figure 5. Exosomes derived from CRC/MDR cells decrease cetuximab sensitivity in a HT-29 cell xenograft tumor model. (A) Tumor volume in each group was measured once every 3 days from day 0 to day 27 after HT-29 cell subcutaneous implantation. (B) Xenografts of HT-29 cells treated with normal saline, cetuximab, exosomes derived from CRC cells combined with cetuximab or exosomes derived from CRC/MDR cells combined with cetuximab. At 4 weeks following subcutaneous implantation, the average tumor volumes in each group were calculated. (C) Tumors were surgically removed from nude mice and weighed after 27 days. (D and E) Representative micrographs of TUNEL labeling of tumors from different treatment groups. Scale bar, 200 μm. The differences among several groups were analyzed using one-way ANOVA followed by Duncan's test. **P<0.01 vs. control; $^{\#\#}$P<0.01 vs. cetuximab + CRC-Exo. CRC, colorectal cancer; exo, exosome; MDR, multidrug resistance.

in patients with mCRC with a lack of response to cetuximab therapy (KRAS mutant group). The results of the present study were in accordance with the findings of a previous study, which reported that cetuximab and panitumumab anti-EGFR therapy significantly improved the survival of patients with KRAS wild-type memorial sloan-kettering cancer center, but was ineffective in the KRAS mutant group (50).

TEM and the assessment of the protein expression levels of exosome specific proteins were performed to characterize exosomes obtained from the culture medium of CRC and CRC/MDR cells. It was demonstrated that exosomes derived from CRC/MDR cells significantly increased resistance to cetuximab treatment in previously cetuximab-sensitive CRC cells. These results were in agreement with the previously reported observation of chemotherapy-induced drug resistance in CRC (51). Furthermore, it has been reported that even with targeted therapeutic agents, such as cetuximab or panitumumab, resistance has also occurred in patients with mCRC (52) and has been implicated as a selection process for CSC-like cells (53).

It has been reported that CSCs maintain the vitality of tumor cell populations via self-renewal and infinite proliferation, which suggests that CSCs can participate in tumorigenesis, invasion and metastasis and have critical significance in chemoradiotherapy resistance (54). Generally, tumor stem cells in organs can be distinguished by surface markers, such as CD24 ligand for P-selectin, CD44 hyaluronan receptor, CD133 five-transmembrane glycoprotein expressed

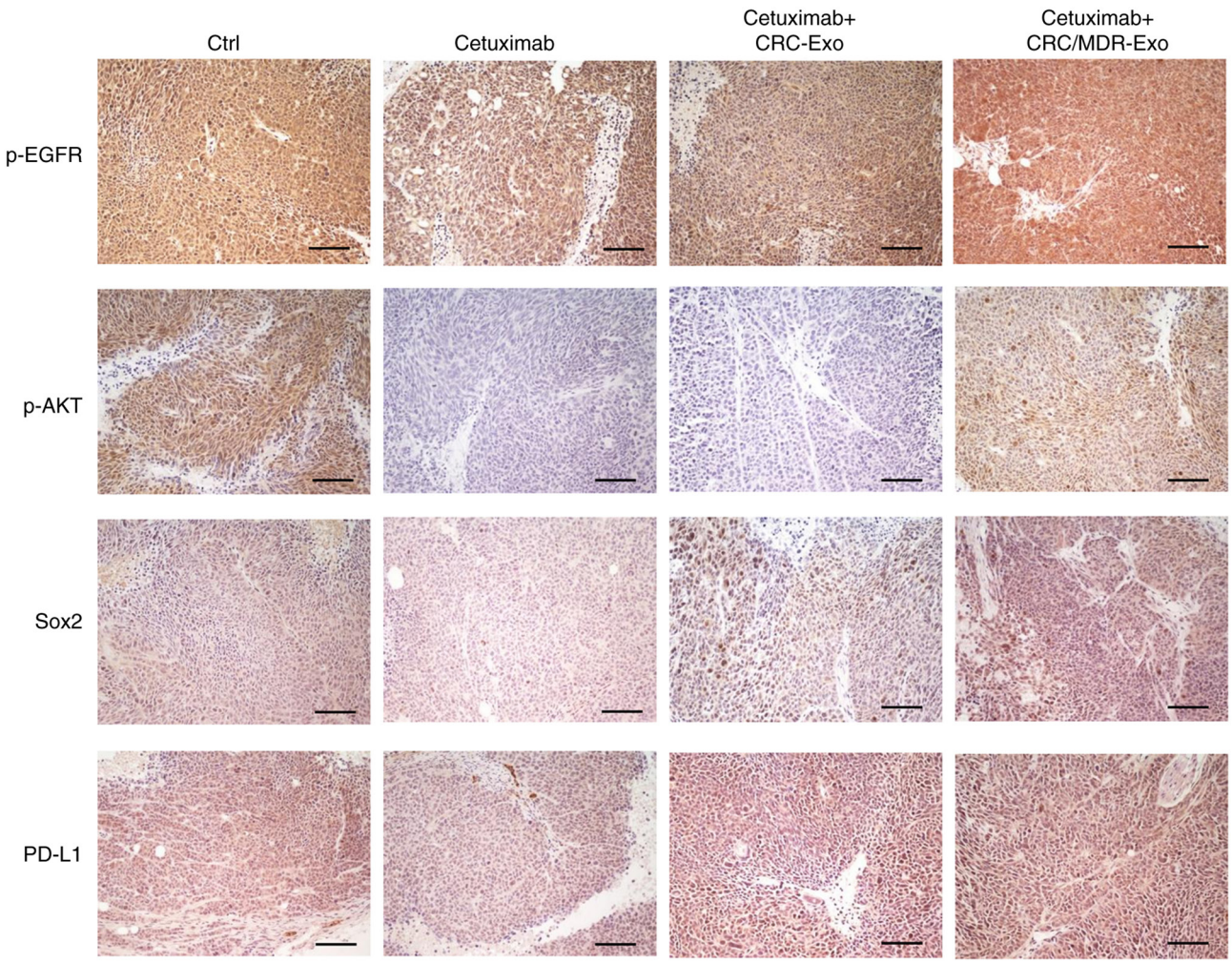

Figure 6. Regulation effect of EGFR-related proteins after exosome treatment in the HT-29 xenograft tumor model. Representative micrographs of xenograft tumor tissues in mice of all treatment groups subjected to immunohistochemistry analysis using p-EGFR, p-AKT, Sox2 and PD-L1 antibodies. Brown staining indicates positive cells. Scale bar, 100 μm. CRC, colorectal cancer; p, phosphorylated; exo, exosome; MDR, multidrug resistance; PD-L1, programmed death-ligand 1.

on the cell surface and epithelial cell adhesion molecule, as a side population of cells with ABC transporters and aldehyde dehydrogenase activity (55). In the present study, both HT-29 and Caco-2 cells consistently demonstrated several CSC-like features, such as an enhanced ability to generate tumor spheres *in vitro* and enhanced tumorigenic ability *in vivo*.

Aberrant Sox2 expression is associated with numerous malignancies and has well-characterized roles in tumor growth, metastasis and drug resistance (56). Emerging evidence has reported that inhibition of PI3K signaling decreases the protein expression levels of Sox2 in CSCs, which suggests that PI3K/mTOR inhibition may successfully circumvent cetuximab resistance via the downregulation of Sox2 and the modulation of downstream transcriptional programs (57,58). In the present study, Sox2 and PD-L1 protein expression levels in Caco-2 cells were related to the response to CRC/MDR-exosomes. Meanwhile, based on the morphology of sphere samples, cell stemness was demonstrated to be markedly increased in cells treated with exosomes from CRC/MDR cells compared with untreated controls, which suggested that anti-EGFR therapy resistance could be related to the change of the TME after chemotherapy resistance. The TME in CRC may potentially disrupt the downstream signal transduction of anti-EGFR therapy, which renders the wild-type KRAS CRC resistant to cetuximab. The present study revealed that CRC/MDR-exosomes could activate the phosphorylation of components of the PI3K/AKT signaling pathway in HT-29 cells and regulate the Sox2-mediated activity of stem cells in Caco-2 cells. Numerous clinical investigations have reported that even with targeted therapeutic agents such as cetuximab or panitumumab, resistance has developed in patients with mCRC and therefore has been implicated as a selection process for CSC-like cells (49,59).

In our previous study, it was reported that elevated protein levels of PI3K and AKT were observed in MDR colorectal cancer cells compared with in sensitive cancer cells (57). This suggests a major resistance mechanism in PI3K/AKT-activated protein kinase (MAPK)-targeted therapies in CRC. Moreover, the previous study suggests that the activation of a non-canonical and independent PI3K/AKT signaling pathway, which involved the overexpression of Sox2 and PD-L1 mediated the activation of tumor stem cells in CRC (25). However, in the present study that Sox2 and PD-L1 protein expression levels demonstrated different responses to

CRC/MDR-exosomes in different KRAS wild-type cells. A new mechanism that promotes cetuximab resistance progression via CRC/MDR-exosome regulation of the activation of the PI3K/AKT signaling pathway and Sox2 and PD-L1 protein expression levels was proposed in the present study.

It was previously demonstrated that exosome delivery from cisplatin-resistant gastric cancer cells may induce chemoresistance phenotypes in sensitive cancer cells (16). The present study demonstrated that MDR/CRC-exosomes can change the cell proliferation and apoptotic phenotype of cetuximab-sensitive CRC cells. Furthermore, the CRC-exosomes demonstrated a smaller effect on the cell apoptotic phenotype of cetuximab-sensitive CRC cells compared with the MDR/CRC-exosomes. To the best of our knowledge, the present study is the first to document the transmissibility of cetuximab resistance via CRC/MRD-exosomes, not only by the enhanced generation of tumor spheres *in vitro*, but also via enhanced tumorigenic ability *in vivo*. Furthermore, the translational regulation of Sox2 and PD-L1 via the PI3K/AKT signaling pathway was also demonstrated as a response potentially mediated by CRC/MDR-exosomes.

However, the major limitations of the present study include that downstream regulation of PI3K/AKT in cetuximab-sensitive cells was not investigated following treatment with CRC/MDR-exosomes. Furthermore, in clinical applications cetuximab is administered to patients with mCRC, in combination with irinotecan when irinotecan-based therapy has failed (60). It has been reported that patients with KRAS mutant could not benefit from cetuximab; however, a recent clinical study has reported that patients with RAS wild-type tumors derived a significant benefit from the addition of cetuximab to FOLFIRI (fluorouracil, leucovorin, and irinotecan, the first-line treatment of mCRC) (61). Therefore, it is also important to study chemotherapy resistance in KRAS mutants. Although certain factors in drug resistance have previously been widely studied, the findings of the present study present important new possibilities for future clinical application.

Acknowledgements

Not applicable.

Funding

The present study was supported by the National Natural Science Foundation of China (grant nos. 81874399, 81973808 and 82174459), the Science Foundation for Shanghai Committee of Science Project (grant nos. 21S21901400 and 19411972000), Shanghai Municipal Health Commission (grant no. 202140198).

Availability of data and materials

The datasets used and/or analyzed during the current study are available from the corresponding author on reasonable request.

Authors' contributions

ZWe and ZWa performed the experiments. ZL, MZ, YZ, QC, LZ and QT analyzed the data and prepared figures. HS and HZ conceived and designed the experiments, analyzed the data and critically revised the manuscript. ZWe and HS confirm the authenticity of all the raw data. All authors have read and approved the final manuscript.

Ethics approval and consent to participate

This study was approved by the Institutional Animal Care and Use Committee of Shuguang Hospital, Shanghai University of Traditional Chinese Medicine (approval no. PZSHUTCM20 0724027; Shanghai, China). The present study was approved by the Medical Ethics and Human Clinical Trial Committee of the affiliated hospitals, Shanghai University of Traditional Chinese Medicine (approval no. 2020-824-31; Shanghai, China). All of the patients or their parents/guardians provided written informed consent.

Patient consent for publication

Not applicable.

Competing interests

The authors declare that they have no competing interests.

References

1. Mizukami T, Izawa N, Nakajima TE and Sunakawa Y: Targeting EGFR and RAS/RAF signaling in the treatment of metastatic colorectal cancer: From current treatment strategies to future perspectives. Drugs 79: 633-645, 2019.
2. Weng J, Li S, Zhu Z, Liu Q, Zhang R, Yang Y and Li X: Exploring immunotherapy in colorectal cancer. J Hematol Oncol 15: 95, 2022.
3. Kim SY and Kim TW: Current challenges in the implementation of precision oncology for the management of metastatic colorectal cancer. ESMO Open 5: e000634, 2020.
4. Beckler MD, Higginbotham JN, Franklin JL, Ham AJ, Halvey PJ, Imasuen IE, Whitwell C, Li M, Liebler DC and Coffey RJ: Proteomic analysis of exosomes from mutant KRAS colon cancer cells identifies intercellular transfer of mutant KRAS. Mol Cell Proteomics 12: 343-355, 2012.
5. Bellier J, Nokin MJ, Caprasse M, Tiamiou A, Blomme A, Scheijen JL, Koopmansch B, MacKay GM, Chiavarina B, Costanza B, *et al*: Methylglyoxal scavengers resensitize KRAS-mutated colorectal tumors to cetuximab. Cell Rep 30: 1400-1416, 2020.
6. Tak E, Kim M, Cho Y, Choi S, Kim J, Han B, Kim HD, Jang CS, Kim JE, Hong YS, *et al*: Expression of neurofibromin 1 in colorectal cancer and cetuximab resistance. Oncol Rep 47: 15, 2022.
7. Woolston A, Khan K, Spain G, Barber LJ, Griffiths B, Gonzalez-Exposito R, Hornsteiner L, Punta M, Patil Y, Newey A, *et al*: Transcriptomic determinants of therapy resistance and immune landscape evolution during Anti-EGFR treatment in colorectal cancer. Cancer Cell 36: 35-50, 2019.
8. Martinelli E, Ciardiello D, Martini G, Troiani T, Cardone C, Vitiello PP, Normanno N, Rachiglio AM, Maiello E, Latiano T, *et al*: Implementing anti-epidermal growth factor receptor (EGFR) therapy in metastatic colorectal cancer: Challenges and future perspectives. Ann Oncol 31: 30-40, 2020.
9. Mangiapane LR, Nicotra A, Turdo A, Gaggianesi M, Bianca P, Di Franco S, Sardina DS, Veschi V, Signore M, Beyes S, *et al*: PI3K-driven HER2 expression is a potential therapeutic target in colorectal cancer stem cells. Gut 71: 119-128, 2020.
10. Yang YN, Zhang R, Du JW, Yuan HH, Li YJ, Wei XL, Du XX, Jiang SL and Han Y: Predictive role of UCA1-containing exosomes in cetuximab-resistant colorectal cancer. Cancer Cell Int 18: 164, 2018.
11. Zhang Y, Huo L, Wei Z, Tang Q and Sui H: Hotspots and frontiers in inflammatory tumor microenvironment research: A scientometric and visualization analysis. Front Pharmacol 13: 862585, 2022.

12. Touil Y, Igoudjil W, Corvaisier M, Dessein AF, Vandomme J, Monté D, Stechly L, Skrypek N, Langlois C, Grard G, *et al*: Cancer cells escape 5FU chemotherapy-induced cell death by entering stemness and quiescence associated with the c-Yes/YAP axis. Clin Cancer Res 20: 837-846, 2014.
13. Mallini P, Lennard T, Kirby J and Meeson A: Epithelial-to-mesenchymal transition: What is the impact on breast cancer stem cells and drug resistance. Cancer Treat Rev 40: 341-348, 2014.
14. Yin Z, Yu M, Ma T, Zhang C, Huang S, Karimzadeh MR, Momtazi-Borojeni AA and Chen S: Mechanisms underlying low-clinical responses to PD-1/PD-L1 blocking antibodies in immunotherapy of cancer: A key role of exosomal PD-L1. J Immunother Cancer 9: e001698, 2021.
15. Ji Q, Zhou L, Sui H, Yang L, Wu X, Song Q, Jia R, Li R, Sun J, Wang Z, *et al*: Primary tumors release ITGBL1-rich extracellular vesicles to promote distal metastatic tumor growth through fibroblast-niche formation. Nat Commun 11: 1211, 2020.
16. Sun MY, Xu B, Wu QX, Chen WL, Cai S, Zhang H and Tang QF: Cisplatin-resistant gastric cancer cells promote the chemoresistance of cisplatin-sensitive cells via the exosomal RPS3-mediated PI3K-Akt-Cofilin-1 signaling axis. Front Cell Dev Biol 9: 618899, 2021.
17. Tan Z, Gao L, Wang Y, Yin H, Xi Y, Wu X, Shao Y, Qiu W, Du P, Shen W, *et al*: PRSS contributes to cetuximab resistance in colorectal cancer. Sci Adv 6: eaax5576, 2020.
18. Cremolini C, Rossini D, Dell'Aquila E, Lonardi S, Conca E, Del Re M, Busico A, Pietrantonio F, Danesi R, Aprile G, *et al*: Rechallenge for patients with RAS and BRAF wild-type metastatic colorectal cancer with acquired resistance to first-line cetuximab and irinotecan: A phase 2 single-arm clinical trial. JAMA Oncol 5: 343-350, 2019.
19. Chinese Society Of Clinical Oncology Csco Diagnosis And Treatment Guidelines For Colorectal Cancer Working Group: Diagnosis and treatment guidelines for colorectal cancer working group CSOCOC: Chinese society of clinical oncology (CSCO) diagnosis and treatment guidelines for colorectal cancer 2018 (English version). Chin J Cancer Res 31: 117-134, 2019.
20. Edge SB, Byrd DR, Compton CC, Fritz AG, Greene FL and Trotti A (eds): AJCC cancer staging manual. 7th edition. Springer, New York, NY, 2010.
21. Karnofsky DA, Abelmann WH, Craver LF, Burchenal JH: The use of the nitrogen mustards in the palliative treatment of carcinoma-with particular reference to bronchogenic carcinoma. Cancer 1: 634-656, 1948.
22. Junjie P, Ji Z and Fangqi L: Chinese expert consensus on the diagnosis and treatment of locally advanced rectal cancer. Chin J Cancer 1: 41-80, 2017 (In Chinese).
23. National Health Commission of the People's Republic of China: Chinese Protocol of Diagnosis and Treatment of Colorectal Cancer (2020 edition). Zhonghua Wai Ke Za Zhi 58: 561-585, 2020 (In Chinese).
24. Lu H, Sun J, Xu JH and Fan ZZ: Establishment of HCT116/L-OHP in oxaliplatin-resistant cells in human colon cancer. Tumors 31: 675-681, 2011.
25. Sui H, Pan SF, Feng Y, Jin BH, Liu X, Zhou LH, Hou FG, Wang WH, Fu XL, Han ZF, *et al*: Zuo Jin Wan reverses P-gp-mediated drug-resistance by inhibiting activation of the PI3K/Akt/NF-κB pathway. BMC Complement Altern Med 14: 279, 2014.
26. Sui H, Zhou L, Zhang Y, Huang JP, Liu X, Ji Q, Fu XL, Wen HT, Chen ZS, Deng WL, *et al*: Evodiamine suppresses ABCG2 mediated drug resistance by inhibiting p50/p65/NF-κB pathway in colorectal cancer. J Cell Biochem 117: 1471-1481, 2016.
27. Wang Z, Sun X, Feng Y, Liu X, Zhou L, Sui H, Ji Q, E Q, Chen J, Wu L and Li Q: Dihydromyricetin reverses MRP2-mediated MDR and enhances anticancer activity induced by oxaliplatin in colorectal cancer cells. Anticancer Drugs 28: 281-288, 2017.
28. Kim SA, Park H, Kim KJ, Kim JW, Sung JH, Nam M, Lee JH, Jung EH, Suh KJ, Lee JY, *et al*: Cetuximab resistance induced by hepatocyte growth factor is overcome by MET inhibition in KRAS, NRAS, and BRAF wild-type colorectal cancers. J Cancer Res Clin Oncol 148: 2995-3005, 2022.
29. Chu YC, Tsai TY, Yadav VK, Deng L, Huang CC, Tzeng YM, Yeh CT and Chen MY: 4-Acetyl-Antroquinonol B improves the sensitization of cetuximab on both kras mutant and wild type colorectal cancer by modulating the expression of Ras/Raf/miR-193a-3p signaling axis. Int J Mol Sci 22: 7508, 2021.
30. Li F, Zhan L, Dong Q, Wang Q, Wang Y, Li X, Zhang Y and Zhang J: Tumor-derived exosome-educated hepatic stellate cells regulate lactate metabolism of hypoxic colorectal tumor cells via the IL-6/STAT3 pathway to confer drug resistance. Onco Targets Ther 13: 7851-7864, 2020.
31. Sun MY, Zhang H, Tao J, Ni ZH, Wu QX and Tang QF: Expression and biological function of rhotekin in gastric cancer through regulating p53 pathway. Cancer Manag Res 11: 1069-1080, 2019.
32. Livak KJ and Schmittgen TD: Analysis of relative gene expression data using real-time quantitative PCR and the 2(-Delta Delta C(T)) method. Methods 25: 402-408, 2001.
33. Wang T, Dong J, Yuan X, Wen H, Wu L, Liu J, Sui H and Deng W: A new chalcone derivative C49 reverses doxorubicin resistance in MCF-7/DOX cells by inhibiting P-glycoprotein expression. Front Pharmacol 12: 653306, 2021.
34. Liu L, Salnikov AV, Bauer N, Aleksandrowicz E, Labsch S, Nwaeburu C, Mattern J, Gladkich J, Schemmer P, Werner J and Herr I: Triptolide reverses hypoxia-induced epithelial-mesenchymal transition and stem-like features in pancreatic cancer by NF-κB downregulation. Int J Cancer 134: 2489-2503, 2014.
35. Wang J, Guo LP, Chen LZ, Zeng YX and Lu SH: Identification of cancer stem cell-like side population cells in human nasopharyngeal carcinoma cell line. Cancer Res 67: 3716-3724, 2007.
36. Elston CW and Ellis IO: Pathological prognostic factors in breast cancer. I. The value of histological grade in breast cancer: Experience from a large study with long-term follow-up. Histopathology 19: 403-410, 1991.
37. Bauman JE and Grandis JR: Targeting secondary immune responses to cetuximab: CD137 and the outside story. J Clin Invest 124: 2371-2375, 2014.
38. Whiteside TL: Exosomes and tumor-mediated immune suppression. J Clin Invest 126: 1216-1223, 2016.
39. Binenbaum Y, Fridman E, Yaari Z, Milman N, Schroeder A, David GB, Shlomi T and Gil Z: Transfer of miRNA in macrophage-derived exosomes induces drug resistance in pancreatic adenocarcinoma. Cancer Res 78: 5287-5299, 2018.
40. Witwer KW, Buzás EI, Bemis LT, Bora A, Lässer C, Lötvall J, Nolte-'t Hoen EN, Piper MG, Sivaraman S, Skog J, *et al*: Standardization of sample collection, isolation and analysis methods in extracellular vesicle research. J Extracell Vesicles 27: 2, 2013.
41. Yonesaka K, Zejnullahu K, Okamoto I, Satoh T, Cappuzzo F, Souglakos J, Ercan D, Rogers A, Roncalli M, Takeda M, *et al*: Activation of ERBB2 signaling causes resistance to the EGFR directed therapeutic antibody cetuximab. Sci Transl Med 3: 99ra86, 2011.
42. Duan H, Liu Y, Gao Z and Huang W: Recent advances in drug delivery systems for targeting cancer stem cells. Acta Pharm Sin B 11: 55-70, 2021.
43. Zhao JJ, Lin J, Zhu D, Wang X, Brooks D, Chen M, Chu ZB, Takada K, Ciccarelli B, Admin S, *et al*: miR-30-5p functions as a tumor suppressor and novel therapeutic tool by targeting the oncogenic Wnt/β-catenin/BCL9 pathway. Cancer Res 74: 1801-1813, 2014.
44. Yun JH, Kim KA, Yoo G, Kim SY, Shin JM, Kim JH, Jung SH, Kim J and Nho CW: Phenethyl isothiocyanate suppresses cancer stem cell properties in vitro and in a xenograft model. Phytomedicine 30: 42-49, 2017.
45. Han Y, Peng Y, Fu Y, Cai C, Guo C, Liu S, Li Y, Chen Y, Shen E, Long K, *et al*: MLH1 deficiency induces cetuximab resistance in colon cancer via Her-2/PI3K/AKT signaling. Adv Sci (Weinh) 7: 2000112, 2020.
46. Li H, Zhou L, Zhou J, Li Q and Ji Q: Underlying mechanisms and drug intervention strategies for the tumour microenvironment. J Exp Clin Cancer Res 40: 97, 2021.
47. Ribatti D, Mangialardi G and Vacca A: Stephen Paget and the 'seed and soil' theory of metastatic dissemination. Clin Exp Med 6: 145-149, 2006.
48. Lièvre A, Bachet JB, Boige V, Cayre A, Corre DL, Buc E, Ychou M, Bouché O, Landi B, Louvet C, *et al*: Kras mutations as an independent prognostic factor in patients with advanced colorectal cancer treated with cetuximab. J Clin Oncol 26: 374-379, 2008.
49. Formica V, Sera F, Cremolini C, Riondino S, Morelli C, Arkenau HT and Roselli M: KRAS and BRAF mutations in Stage II and III colon cancer: A systematic review and meta-analysis. J Natl Cancer Inst 114: 517-527, 2022.
50. Cai MH, Xu XG, Yan SL, Sun Z, Ying Y, Wang BK and Tu YX: Regorafenib suppresses colon tumorigenesis and the generation of drug resistant cancer stem-like cells via modulation of miR-34a associated signaling. J Exp Clin Cancer Res 37: 151, 2018.

51. Hsu HC, Thiam TK, Lu YJ, Yeh CY, Tsai WS, You JF, Hung HY, Tsai CN, Hsu A, Chen HC, *et al*: Mutations of KRAS/NRAS/BRAF predict cetuximab resistance in metastatic colorectal cancer patients. Oncotarget 7: 22257-22270, 2016.
52. Lu H, Chen I, Shimoda LA, Park Y, Zhang C, Tran L, Zhang H and Semenza GL: Chemotherapy-induced Ca2+ release stimulates breast cancer stem cell enrichment. Cell Rep 18: 1946-1957, 2017.
53. Cioffi M, D'Alterio C, Camerlingo R, Tirino V, Consales C, Riccio A, Ieranò C, Cecere SC, Losito NS, Greggi S, *et al*: Identification of a distinct population of CD133+CXCR4+ cancer stem cells in ovarian cancer. Sci Rep 5: 10357, 2015.
54. Steinbichler TB, Dudás J, Skvortsov S, Ganswindt U, Riechelmann H and Skvortsova II: Therapy resistance mediated by cancer stem cells. Semin Cancer Biol 53: 156-167, 2018.
55. Wuebben EL and Rizzino A: The dark side of SOX2: Cancer- a comprehensive overview. Oncotarget 8: 44917-44943, 2017.
56. Keysar SB, Le PN, Miller B, Jackson BC, Eagles JR, Nieto C, Kim J, Tang B, Glogowska MJ, Morton JJ, *et al*: Regulation of head and neck squamous cancer stem cells by PI3K and SOX2. J Natl Cancer Inst 109: djw189, 2016.
57. Bouhaddou M, Lee RH, Li H, Bhola NE, O'Keefe RA, Naser M, Zhu TR, Nwachuku K, Duvvuri U, Olshen AB, *et al*: Caveolin-1 and Sox-2 are predictive biomarkers of cetuximab response in head and neck cancer. JCI Insight 6: e151982, 2021.
58. Rothenberg SM, Concannon K, Cullen S, Boulay G, Turke AB, Faber AC, Lockerman EL, Rivera MN, Engelman JA, Maheswaran S and Haber DA: Inhibition of mutant EGFR in lung cancer cells triggers SOX2-FOXO6-dependent survival pathways. Elife 4: e06132, 2015.
59. Liu K, Lin B, Zhao M, Yang X, Chen M, Gao A, Liu F, Que J and Lan X: The multiple roles for Sox2 in stem cell maintenance and tumorigenesis. Cell Signal 25: 1264-1271, 2013.
60. Cunningham D, Humblet Y, Siena S, Khayat D, Bleiberg H, Santoro A, Bets D, Mueser M, Harstrick A, Verslype C, *et al*: Cetuximab monotherapy and cetuximab plus irinotecan in irinotecan-refractory metastatic colorectal cancer. N Engl J Med 351: 337-345, 2004.
61. Van Cutsem E, Lenz HJ, Köhne CH, Heinemann V, Tejpar S, Melezínek I, Beier F, Stroh C, Rougier P, van Krieken JH and Ciardiello F: Fluorouracil, leucovorin, and irinotecan plus cetuximab treatment and RAS mutations in colorectal cancer. J Clin Oncol 33: 692-700, 2015.